

New tests of the correspondence between unitary eigenvalues and the zeros of Riemann's zeta function

Marc Coram and Persi Diaconis

Department of Statistics, Stanford, CA 94305, USA

Received 1 July 2002, in final form 6 November 2002

Published 12 March 2003

Online at stacks.iop.org/JPhysA/36/2883

Abstract

This paper presents some new statistical tests and new conjectures regarding the correspondence between the eigenvalues of random unitary matrices and the zeros of Riemann's zeta function. Global features such as the trace and number of eigenvalues in intervals are compared. Our results show satisfying match-ups between the two domains. They give examples of large natural datasets that follow classical distributions to high accuracy.

PACS numbers: 02.10.Yn, 02.10.De

1. Introduction

The Riemann hypothesis is one of the outstanding problems of modern mathematics. It posits that all of the complex zeros of the zeta function $\sum_{n=1}^{\infty} \frac{1}{n^s}$ with real part between 0 and 1 lie on the line $\text{Re}(s) = \frac{1}{2}$. Polya and Hilbert suggested that one way to prove the Riemann hypothesis is to find a self-adjoint operator whose eigenvalues are the zeros of the zeta function (suitably shifted). This introduced a connection between zeros and eigenvalues which is actively being pursued [35].

There is now considerable evidence that there is a close connection between the zeta zeros and the eigenvalues of typical *unitary matrices*. Figure 1, based on the work of Odlyzko [46], compares the spacings of consecutive zeros (based on 10^4 zeros starting with 10^{12}), scaled to have density one, with the spacings of consecutive eigenvalues of randomly chosen matrices in the unitary group, U_n , for $n = 24$. Also shown is the Wigner surmise: $\frac{32}{\pi^2} x^2 \exp(-\frac{4}{\pi} x^2)$ [42]. The fit is good, and Odlyzko's work shows that the fit gets better for higher zeros.

Spacings capture *local* features of the zeros and eigenvalues. In the paper we compare *global* features of the eigenvalues of typical elements of U_n to the zeros of the zeta function.

1.1. Method of comparison

Recall that the Riemann zeta function may be defined by $\zeta(s) = \sum_{n=1}^{\infty} \frac{1}{n^s}$ for $\text{Re}(s) > 1$. By analytic continuation, it extends to the entire complex plane (*sans* a simple pole at 1). The zeros

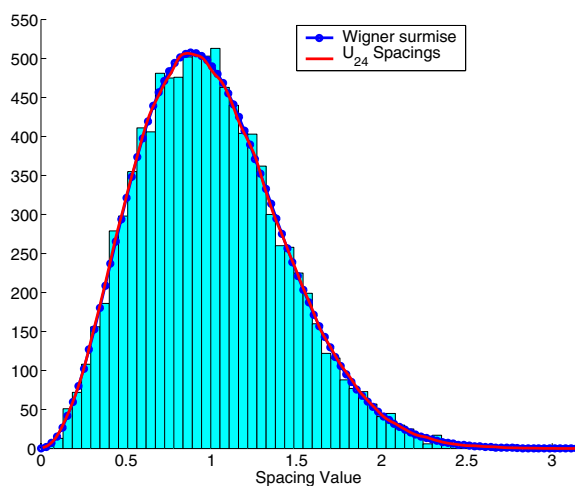


Figure 1. Histogram of zeta zeros spacings scaled to have mean 1 and matched spacing pdfs for U_{24} (empirical) and the Wigner surmise.

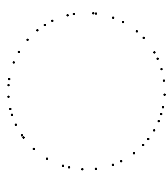


Figure 2. Unitary eigenvalues.



Figure 3. Uniform points.

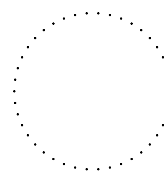


Figure 4. Picket fence model.

in the critical strip $0 \leq \operatorname{Re}(s) \leq 1$, $\operatorname{Im}(s) > 0$ have been intensively studied. Good references for what is currently known are Edwards [23], Titchmarsh [56] and Karatsuba-Voronin [34]. It is known, for example, that the zeta function has trivial zeros at $-2, -4, -6, \dots$ and that all nontrivial zeros are symmetric about the line $\operatorname{Re}(s) = 1/2$. The Riemann hypothesis is that all nontrivial zeros are on this line.

If $N(T)$ is the number of zeros in the strip up to height T , it is known [56] that

$$N(T) = \frac{T}{2\pi} \log \frac{T}{2\pi e} + O(\log(T)). \quad (1)$$

Thus, the zeros at height T have the approximate density $\frac{1}{2\pi} \log \frac{T}{2\pi}$.

The unitary group U_n is the group of $n \times n$ complex matrices M such that $MM^* = I$. Such a matrix has eigenvalues $\{e^{i\theta_1}, \dots, e^{i\theta_n}\}$. We will choose matrices from Haar measure on U_n [22]. Figure 2 shows the eigenvalues of a random matrix drawn from U_{42} . In contrast, figure 3 shows 42 points put down at random on the unit circle. It is evident that the unitary eigenvalues are much more neatly distributed than uniform points. However, they are not as regular as the evenly spaced ‘picket fence’ points in figure 4. The eigenvalues of random unitary matrices have density $\frac{n}{2\pi}$. Equating unitary and zeta densities suggests that we match n with $\lfloor \log \frac{T}{2\pi} \rfloor$.

In the data used below we consider 50 000 consecutive zeros starting around the $10^{20} + 271\,959\,460$ th zero. According to Odlyzko [47] the 10^{20} th zero equals $\frac{1}{2} + iT_{20}$, with $T_{20} = 15, 202, 440, 115, 930, 747, 268.6290299 \dots \doteq 0.15 \times 10^{20}$. Thus $\log \frac{T}{2\pi} \doteq 42.3$. Accordingly, in the following, the zeros at height T_{20} will be compared with random elements in U_{42} .

To compare the eigenvalues of random unitary matrices with the zeros of the Riemann zeta function we put the zeros onto the unit circle according to the following procedure: given a list of zeros, we split it up into groups and wrap each group onto the unit circle, being careful to preserve the relative spacings. More precisely, suppose we have zeros Z_1, Z_2, \dots, Z_B of the form $Z_j = \frac{1}{2} + i\tau_j$, $\tau_1 < \tau_2 < \dots < \tau_B$. We form the spacings $\delta_j = \tau_{j+1} - \tau_j$ and split the spacings up into disjoint groups of size n (as discussed, we take $n = 42$). Each group of spacings $\delta_1, \dots, \delta_n$ is mapped onto the unit circle by taking $X_j = \exp\left(2\pi i\left(\frac{\Delta_j}{\Delta_n} + U\right)\right)$, for $1 \leq j \leq n$, where $\Delta_j = \sum_{k=1}^j \delta_k$ is the cumulative sum of the spacings and U is independently generated for each block according to the uniform distribution on $[0, 1)$. U is added to give each block an independent rotation.

1.2. A null hypothesis

We frame the connection between zeta zeros and eigenvalues as a formal statistical hypothesis. To test this hypothesis, we devise several test statistics (functions of the data) whose distribution under the null hypothesis is known. The null hypothesis will be rejected if these statistics take exceptionally large values.

Hypothesis 1.1. *For large T and $B = o(\sqrt{T})$, let $n = \lfloor \log \frac{T}{2\pi} \rfloor$. The $N = \lfloor (B-1)/n \rfloor$ groups of zeros, wrapped around the unit circle, behave like independent draws from Haar measure on U_n .*

In section 2, we compare the distribution of the trace of a random matrix to the 'trace' based on the zeta zeros and find a remarkable goodness of fit. In section 3 we carry out a graphical analysis based on strange correlations for unitary eigenvalues. Again the wrapped zeros show remarkable fit to the predictions of random matrix theory. In section 4 we carry out two further tests of the hypothesis. The first introduces a one-parameter family of alternatives based on Selberg's integral. This produces our only test which casts doubt on the null hypothesis. The second test is a non-parametric Fourier-type test based on symmetric function theory. This global test is shown to have power against nearby alternatives, but again fails to reject the null hypothesis.

In section 5 we investigate the independence of successive blocks of zeta zeros. There is substantial negative correlation between successive spacings. A subsampling analysis shows that this does not materially affect our previous conclusions, but it leads to a modified hypothesis. A final section draws some conclusions.

The results in this paper are based on our new wrapping technique which allows comparison of the zeta zeros (on a line) with unitary eigenvalues (on a circle). We hope our findings will also be of interest as natural real, large datasets where classical models (e.g., the standard exponential distribution of section 2) provide a good fit to data. As far as we know, the tests presented here are the first careful statistical tests of a well-specified hypothesis for this problem. As discussed in the literature review, random matrix theory is believed to fit a rich variety of datasets in physics. Our tests and data-analytic procedures could prove useful here as well.

The present paper uses probabilistic techniques to analyse patently non-random data. Of course, the digits of π and e are classical cases where such tests have been carried out. Chaotic dynamical systems offer further examples.

1.3. Previous literature

Random matrix theory uses the eigenvalues of various ensembles of random matrices to model natural phenomena. Perhaps the earliest work in this area is statistical in nature and studies covariance matrices. Bai [3] and Johnstone [33] give up to date reviews of this work. Wigner and Dyson suggest random matrix models for a variety of particle scattering data. This started an avalanche of theoretical and applied work surveyed in Bohigas [8], Mehta [42], Hejhal *et al* [31] and Guhr *et al* [29]. The last paper has a bibliography of 816 items.

One exciting development, the Bohigas conjecture [8], suggests that random matrix statistics apply to the eigenvalues of the Laplacian on two-dimensional domains, provided that billiards on these domains are chaotic. Empirical tests of the Bohigas conjecture have used spacings. We hope to apply our wrapping ideas to compare these data with unitary eigenvalues.

Connections between random matrix theory and the zeta zeros begin with the work of Montgomery [43] and Odlyzko [46]. Berry [5] and Bogomolny-Keating [7] have developed amazingly accurate models for two-point correlations. Their work shows that random matrix theory alone is not sufficient to capture global properties of zeta zeros such as two-point correlations; information about primes is needed as well. While much of this work is data analytic and heuristic, there is much that can be proved. Katz and Sarnak [35] and Rudnick and Sarnak [50] offer proofs of many findings. Berry and Keating [6] and Conrey [12] offer up to date surveys.

Keating and Snaith [38, 39] have pioneered a fresh investigation based on matching zeros at height T to the eigenvalues in U_n with n of order $\log(T)$. They have found a good match of theory to data and used random matrix theory to give remarkable, precise conjectures on the average order of powers of the zeta function on the critical line. Conrey and Gonek [14] offer number theoretic background showing the usefulness of the correspondence between the zeta function and the characteristic polynomial of a random element of U_n . More recently, Conrey *et al* [13] have used random matrix theory to give detailed heuristic asymptotic expansions for zeta moments and Diaconu *et al* [17] have complemented these with heuristics based on number theory.

To summarize, previous tests of random matrix theory have used local properties, such as spacings, or global properties, such as the variance. For local properties, random matrix theory provides a remarkable fit to the zeta zeros. For global properties, the correspondence can break down. The present paper studies intermediate properties where the correspondence seems to hold.

2. A trace test

This section compares the distribution of the trace of a random matrix with a parallel statistic for the Riemann zeros.

For M chosen uniformly in U_n , Diaconis and Mallows [18] proved that the trace of M has an approximate complex normal distribution. This was refined by Diaconis and Shahshahani [22], Stein [55] and Johansson [32]. One consequence of Johansson's work is the following approximation showing that the norm of the trace has an exponential distribution to remarkable approximation.

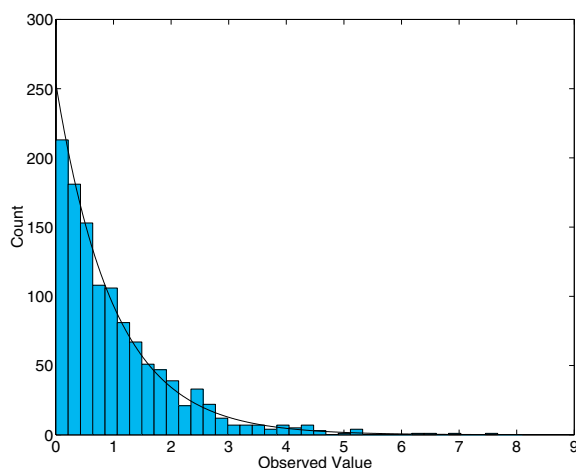


Figure 5. Zeta function based norm-squared-‘traces’ with standard exponential pdf superimposed.

Theorem 2.1. *There are positive c, δ such that for all $n \geq 1$, for M chosen uniformly in U_n and for all $t \geq 0$,*

$$|P(|\text{tr } M|^2 \geq t) - e^{-t}| \leq cn^{-\delta n}. \tag{2}$$

To compare theorem 2.1 with the zeta zeros, 50 000 consecutive zeros of the zeta function starting near zero number $10^{20} + 271\,959\,460$ were broken into 1190 blocks of length 42 and wrapped around the unit circle as explained in section 1.1. For each block, the ‘trace’ was computed, i.e. the sum of the 42 complex values on the circle. We denote the norm squared of these sums by W_i for i from 1 to 1190. The W would be distributed according to the exponential distribution with mean 1 (density e^{-x}) to very good approximation if they were actually formed from the trace of random matrices in U_n , giving us a natural test of the match-up.

Figure 5 shows a histogram and figure 6 a probability plot of these values plotted against an exponential. The fit seems good in both cases, but both plots have their deficiencies. The probability plot, for example, accentuates the tail variability at the cost of showing variation for more central values.

We carried out two formal goodness-of-fit tests to compare $\{W_j\}_{j=1}^{1190}$ with the exponential distribution. The first test is the Anderson–Darling test [1]. This is based on

$$A^2 = \int_0^\infty \frac{(\hat{F}(t) - F(t))^2}{F(t)(1 - F(t))} dF(t)$$

with $F(t) = 1 - e^{-t}$ the distribution function of the exponential distribution and $\hat{F}(t) = \frac{1}{1190} |\{j : W_j \leq t\}|$. In the experiment $A^2 = 1.1050$. The distribution of A^2 is known under the null hypothesis and results of D’Agostino and Stephens [16] give $P(A^2 \leq 1.1) \doteq 0.69$. We see that the observed value of A^2 lies squarely in the centre of the distribution so that the null hypothesis is not rejected in this case.

The second test carried out is Neyman’s smooth test ([45, 16], p 351). This transforms the data to $[-\frac{1}{2}, \frac{1}{2}]$ via $U_j = 1 - e^{-W_j - \frac{1}{2}}$. Under the null hypothesis, $\{U_j\}$ are independent

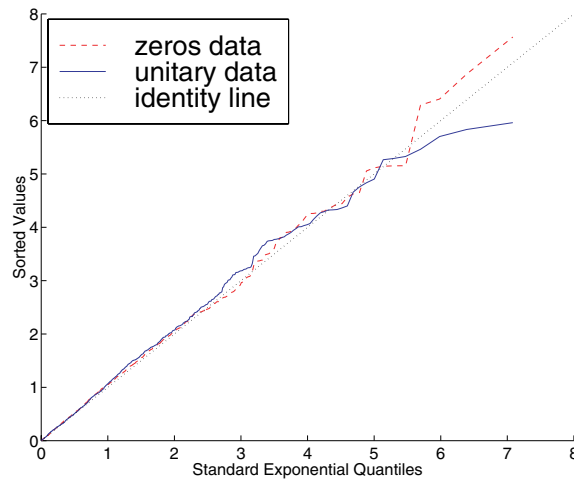


Figure 6. Probability plot of norm-squared-‘traces’ relative to the standard exponential distribution.

uniform variates on $[-\frac{1}{2}, \frac{1}{2}]$. Neyman’s test computes the average of the first four orthogonal polynomials p_i (the Legendre polynomials on $[-\frac{1}{2}, \frac{1}{2}]$) evaluated at these points:

$$S_i = \frac{1}{\sqrt{1190}} \sum_{j=1}^{1190} p_i(U_j) \quad 1 \leq i \leq 4$$

where $p_1(x) = 2\sqrt{3}x$, $p_2(x) = \sqrt{5}(6x^2 - 0.5)$, $p_3(x) = \sqrt{7}(20x^3 - 3x)$, $p_4(x) = 3(70x^4 - 15x^2 + 0.375)$.

Under the null hypothesis, $\{S_i\}_{i=1}^4$ approximately follow the standard normal distribution so that the test statistic $N^* = \sum_{i=1}^4 S_i^2$ has an approximate chi-squared distribution on four degrees of freedom. On the present data $N^* = 2.2848$ and $P(N^* \leq 2.2848) = 0.3165$. So again we fail to reject the null hypothesis.

Fan [24] discusses other tests which, in a sense, interpolate between omnibus tests such as the Anderson–Darling test and Neyman’s smooth test. The idea is to choose a possibly growing number of orthogonal polynomials, where the number chosen is determined by the data. For tests with power against ‘spiky’ alternatives, Fan suggests variants using wavelets.

Of course, there are a huge variety of possible tests (see D’Agostino and Stephens [16] or the work of Verdinelli and Wasserman [57]). Before looking at our data, we choose two well-known, standard tests with a good track record in applied work. We have resisted the temptation to carry out dozens of further tests for fear of contaminating our results.

Note that 1190 is quite a large sample size; goodness-of-fit tests with such sample sizes are notoriously difficult to pass with real data (see Diaconis and Efron [19]). We conclude that the evidence of this section offers strong support for the hypothesis that consecutive blocks of $n = \lfloor \log \frac{T}{2\pi} \rfloor$ zeros starting at height T wrapped around the circle have sums which behave like the trace of independent picks from Haar measure on U_n .

With some thought, however, we can find alternative models for which the trace tests do not have much power of discrimination. The simplest such example is the picket fence model in which n points are first evenly spaced on the unit circle and then each independently perturbed by random noise, where the level of the noise is chosen so that the expected norm squared of the trace is 1. This alternative model may be hard to discriminate because the trace will be approximately normally distributed by the central limit theorem.

For concreteness, to generate a realization from the picket fence model, let $\Theta_j = a_n X_j + j/n + U$ for j from 1 to n , where the X_j are independent standard normal random variables, and U is an independent uniform random variable. We choose $a_n = \frac{1}{2\pi} \sqrt{\log \frac{n}{n-1}}$ so that

$$\mathbf{E} \left| \sum_{j=1}^n e^{2\pi i \Theta_j} \right|^2 = 1.$$

Indeed, upon experimentation, we find that datasets containing 1190 realizations from this picket fence model typically are not rejected by the Anderson–Darling or Neyman smooth tests.

The picket fence model is distinguished from Haar measure through the correlation tests of section 3.3 and through the higher trace tests of section 4.2.

3. Correlations of points in intervals

This section presents a truly counterintuitive property of unitary eigenvalues. The match with the zeta data may be our most surprising finding.

We first explain limiting and fixed n results for the unitary group. Then, the wrapped zeros are compared with the unitary results and good agreement is found. Alternative hypotheses (uniform points and picket fence models) are then considered. Finally, rigorous limiting theorems of Wieand and Selberg are compared.

3.1. Unitary eigenvalues

Wieand [58] studied the joint distribution of eigenvalues of random elements of U_n in several intervals on the unit circle. She found that, normalized by mean and variance, the number of eigenvalues in intervals have an unusual correlation structure. Consider two intervals $(e^{2\pi i \alpha}, e^{2\pi i \beta})$ and $(e^{2\pi i \gamma}, e^{2\pi i \delta})$. In the large n limit, Wieand proved.

Theorem 3.1. *For a uniform random matrix in U_n , the number of eigenvalues in two intervals have the following limiting correlations as n tends to infinity:*

- for disjoint intervals, zero correlation,
- for overlap, $\alpha < \gamma < \beta < \delta$, zero correlation,
- for $\alpha < \beta = \gamma < \delta$, correlation $-\frac{1}{2}$,
- for $\alpha = \gamma < \delta < \beta$, correlation $\frac{1}{2}$,
- For $\alpha = \gamma, \beta = \delta$, correlation 1.

Wieand’s results are described more carefully in section 3.4. To compare with the zeta function, finite n results are needed.

For $0 \leq \theta \leq 1$, let $I(\theta) = (e^{2\pi i \theta}, e^{2\pi i(\theta+\frac{1}{4})})$. This is an arc covering $\frac{1}{4}$ of the unit circle. For a matrix $M \in U_n$ let $A(\theta) = A(\theta, M)$ be the number of eigenvalues of M in $I(\theta)$. We consider

$$R(\theta) = \text{corr}(A(\theta, M), A(0, M)). \tag{3}$$

We carried out a Monte Carlo experiment to determine $R(\theta)$ when M is chosen from Haar measure. This required N independent matrices. As an empirical estimator on the data

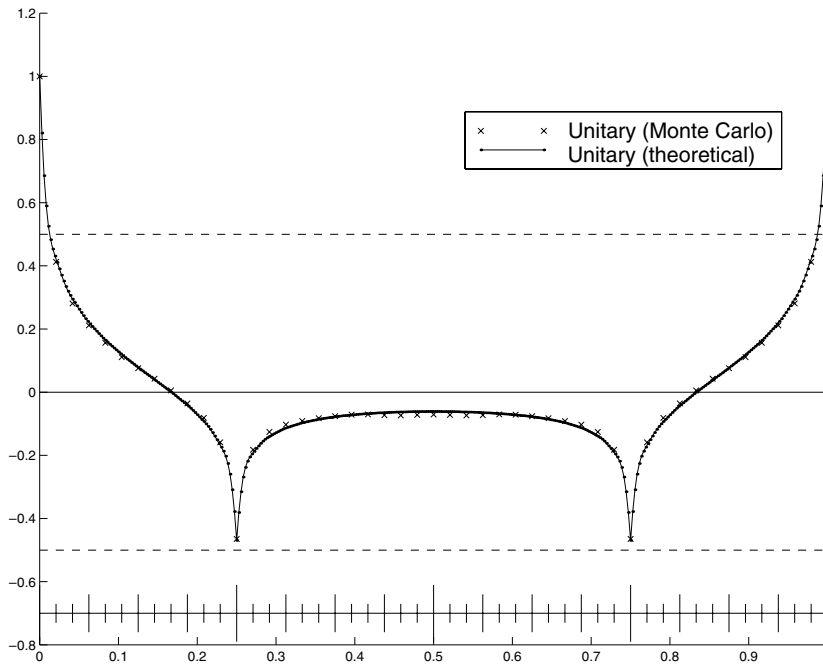


Figure 7. $\hat{R}(\theta)$ versus θ for $N = 1000$ matrices in U_{42} (crosses) with analytical curve (solid) superimposed.

$\{e^{2\pi i\theta_j^{(m)}}\}$ (j from 1 to n , m from 1 to N) we use

$$\hat{R}(\theta) = \frac{\sum_{m=1}^N \int_0^1 \eta_m(t)\eta_m(t+\theta) dt - \mu^2}{\sum_{m=1}^N \int_0^1 \eta_m(t)^2 dt - \mu^2} \tag{4}$$

where $\eta_m(t) = |\{j : e^{2\pi i\theta_j^{(m)}} \in I(t)\}|$ plays the role of $A(\theta, M)$ and $\mu = \frac{n}{4} = \mathbf{E}A(\theta)$.

It is worth noting that this estimator takes advantage of the rotational symmetry of the problem. Each realization of points on the circle is associated with the class, indexed by t , of equally likely realizations that result from rotating by $2\pi t$. Because of this symmetry, and our reasonably large sample size, the resulting empirical correlation curves are more smooth than might otherwise be expected.

Figure 7 shows $\hat{R}(\theta)$ versus θ for $0 \leq \theta \leq 1$. It is based on $N = 1000$ matrices in U_{42} . Of course, when $\theta = 0$, $R(\theta) = 1$. The estimated correlation $\hat{R}(\theta)$ drops close to zero and then further to $-\frac{1}{2}$ at $\theta = \frac{1}{4}$ when the intervals $I(0)$ and $I(\theta)$ have exactly one endpoint in common. For $\frac{1}{4} < \theta < \frac{3}{4}$, the intervals are disjoint, and $\hat{R}(\theta)$ goes back close to 0. Since n is fixed at 42, there is a slight forced negative correlation (if $A(0)$ is large, $A(\theta)$ must be small). At $\theta = \frac{3}{4}$, the intervals again abut and the correlation drops back to $-\frac{1}{2}$. Finally, the correlation climbs back to zero and then to 1 for $\frac{3}{4} < \theta \leq 1$.

Bump *et al* [11] prove

$$\begin{aligned} \frac{\text{cov}(A(0), A(\theta))}{n} &= \left(\frac{1}{4} - \theta\right)_+ + \left(\frac{1}{4} - \theta - 1\right)_+ - \frac{1}{16} \\ &\quad - \sum_{k=1}^n \frac{1 - \frac{k}{n}}{\pi^2 k^2} \left(1 - \cos\left(\frac{k\pi}{2}\right)\right) \cos(2\pi k\theta). \end{aligned}$$

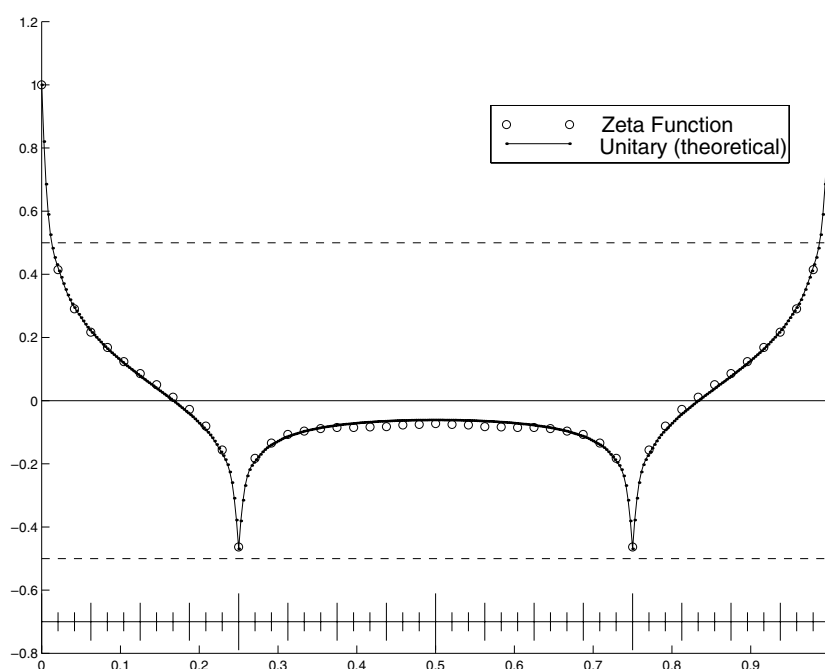


Figure 8. $\hat{R}(\theta)$ versus θ for the zeta function (circles).

Using this gives an analytic expression for $R(\theta)$. As can be seen in figure 7, the analytical expression and the empirical estimate agree very well.

In light of the close match between simulation and theory it is natural to ask, ‘why bother to derive the theory?’ In our work on the correlation plots of figure 9, we initially found a wide discrepancy between the zeta data and the unitary data. For a while, this was one of our most interesting findings and first draft of this paper included a page of discussion. As a routine check we compared the unitary plot based on simulation with the theoretical approximation. They were different, but subsequent runs of the simulation matched the theory. We never located the glitch.

3.2. Zeros of Riemann's zeta function

Odlyzko's zeta data described in section 1 was wrapped around the circle to give 1190 fake sets of eigenvalues. This data was treated as described in section 3.1. Figure 8 shows the unitary and zeta plots superimposed. We also carried out a similar comparison based on correlation between intervals of different lengths. The results for one interval being a quarter circle and the other being a half circle are shown in figure 9. Again the two curves were very close. It seems that the same strange correlations found by Wieand are present in the local structure of the zeta zeros.

3.3. Alternative hypotheses

In this section we test the power of the graphical correlation test of figure 8 against two alternative models.

3.3.1. Uniform points. Under the uniform model n points are independently and uniformly put on the unit circle. This is independently repeated N times and the correlation between

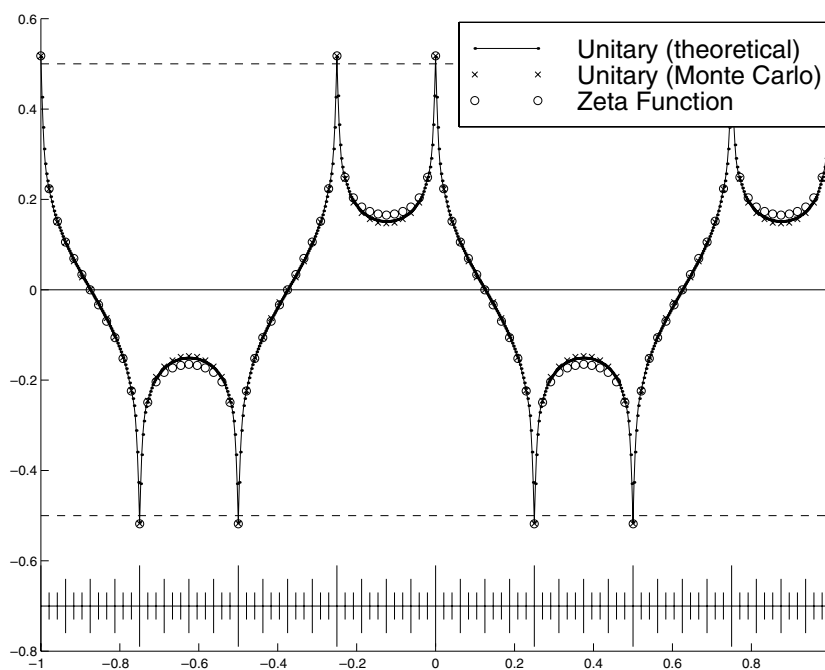


Figure 9. Correlation for unequal intervals.

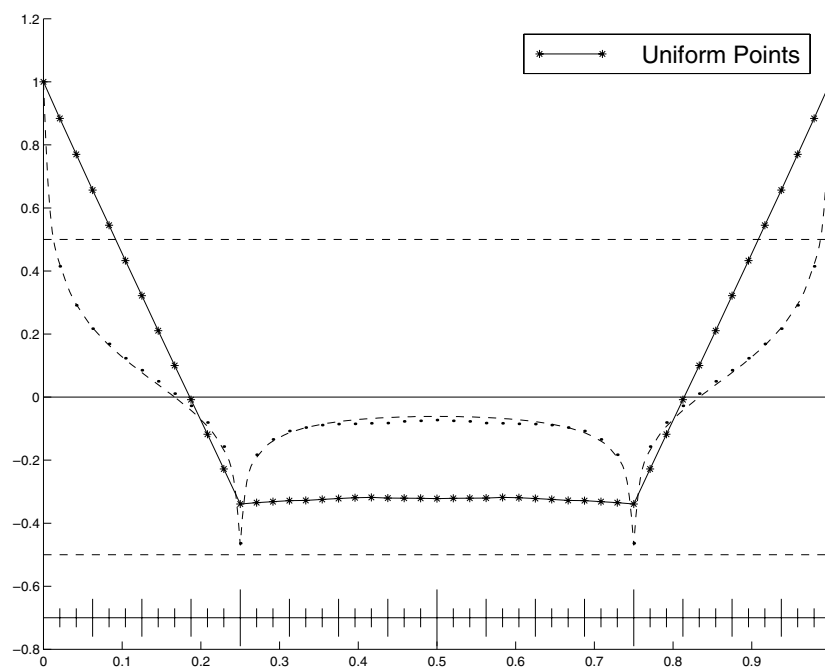


Figure 10. Uniform points.

$A(0)$ and $A(\theta)$ is computed via definition (4). The result shown in figure 10 shows marked deviations from the unitary and zeta function correlations.

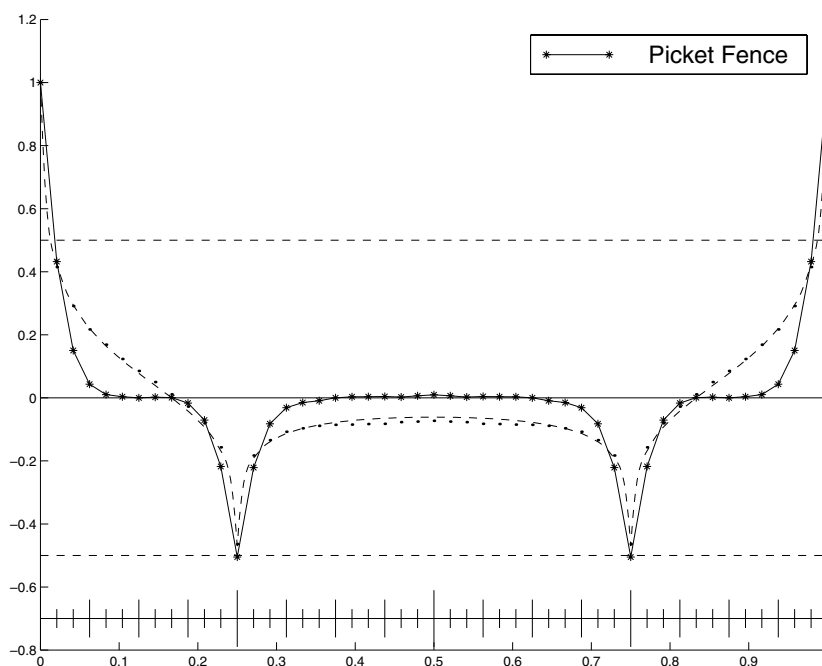


Figure 11. Picket fence.

For the uniform model it is straightforward to derive an analytic expression for the correlations. Let

$$\hat{C}(\theta) = \frac{\mathbf{E}(N(0) - \bar{N}(0))(N(\theta) - \bar{N}(\theta))}{\mathbf{E}(N(0) - \bar{N}(0))^2}$$

with $N(\theta)$ the number of points in $(e^{2\pi i\theta}, e^{2\pi i(\theta+\pi/4)})$.

Proposition 3.2. *Under the uniform model, for $0 \leq \theta \leq 1$,*

$$\hat{C}(\theta) = \frac{16}{3} \left\{ \left(\frac{1}{4} - \theta\right)_+ + \left(\theta - \frac{3}{4}\right)_+ - \frac{1}{16} \right\}.$$

We have compared proposition 3.2 with the Monte Carlo data underlying figure 10, and found an excellent fit.

3.3.2. Picket fence. Under a picket fence model, n points are put on the unit circle with exactly equal spacing $\frac{2\pi}{n}$ from a uniformly chosen start. The points are then perturbed by adding independent random noise. Recall that data generated from this model passes the trace test of section 2. For the present test, N independent repetitions are generated. The result is shown in figure 11 for $n = 42$, $N = 1000$, and Gaussian noise centred at each point with standard deviation $a_{42} = \frac{1}{2\pi} \sqrt{\log \frac{n}{n-1}} = 0.0247$ (as defined at the end of section 2). This is clearly different from the unitary and zeta data, but closer to these than the uniform model. This shows that the graphical trace test can detect small departures from the null. Daley has suggested using a nonparametric perturbation instead of this Gaussian one; we have not attempted this.

3.4. On limiting normality

Wieand [58] seems to have been the first to prove that if M is chosen uniformly in U_n , then the number of eigenvalues of M that lie in the intervals I_1, I_2, \dots, I_n , normalized by their means and variances, have an asymptotic Gaussian distribution with mean zero and correlations given by theorem 3.1. Earlier, Costin and Lebowitz [15] proved a similar Gaussian limit theorem for a random Hermitian matrix (GUE). Soshnikov [53] has shown that their method can be adapted to prove Gaussian limit theorems for a variety of matrix ensembles: basically, those with k -point marginals representable as determinants. This gives a different proof of Wieand’s result and extensions to much more general interval lengths. For comparison with Selberg’s result we state the single interval theorem here.

Theorem 3.3 (Wieand). *Let M be chosen uniformly in the unitary group U_n . Fix $0 \leq \alpha < \beta < 1$. Let $N(\alpha, \beta)$ be the number of eigenvalues of M in $(e^{2\pi i\alpha}, e^{2\pi i\beta})$. Then as n tends to infinity, for all fixed real x ,*

$$P \left(\frac{N(\alpha, \beta) - n|\beta - \alpha|}{\frac{1}{\pi} \sqrt{\log n}} \leq x \right) \rightarrow \frac{1}{\sqrt{2\pi}} \int_{-\infty}^x e^{-\frac{s^2}{2}} ds.$$

Selberg [51] proved several results about the distribution of the number of zeta zeros in a randomly chosen interval. Selberg’s limit results have been compared with data and with unitary eigenvalues by Keating and Snaith [38] who found the actual distribution (based on data) closer to the unitary ensemble than to the limiting normal approximation. In a remarkable contribution, they used exact calculation from the unitary ensemble to predict the average order of powers of $\zeta(s)$ on the critical line; the predictions match previously proved results and give striking new conjectures.

For comparison, here is Selberg’s limiting result.

Theorem 3.4 (Selberg). *For t chosen uniformly in $[0, T)$, let $N(t)$ be the number of zeros in the critical strip up to height t . Then, as $T \nearrow \infty$*

$$P \left(\frac{N(t) - \frac{t}{2\pi} \log\left(\frac{t}{2\pi e}\right)}{\sqrt{\frac{1}{2\pi^2} \log \log T}} \leq x \right) \rightarrow \frac{1}{\sqrt{2\pi}} \int_{-\infty}^x e^{-\frac{s^2}{2}} ds.$$

While both theorems 3.3 and 3.4 have normal limits, Wieand’s theorem involves centring about $n|\beta - \alpha|$ while Selberg’s theorem involves centring about the random term $\frac{t}{2\pi} \log\left(\frac{t}{2\pi e}\right)$.

A referee has pointed to work of Fujii [31, pp 219–67] which proves that for fixed $h > 0$, as $T \nearrow \infty$

$$\frac{1}{T} P \left\{ T \leq t \leq 2T : \frac{N(t+h) - N(t) - \frac{h}{2\pi} \log \frac{t}{2\pi}}{\sqrt{(\log \log T)/\pi^2}} \leq x \right\} \rightarrow \frac{1}{\sqrt{2\pi}} \int_{-\infty}^x e^{-s^2/2} ds.$$

This may be a closer link to Wieand’s result.

We conclude this section by an empirical comparison of the distribution of eigenvalues and zeros in an interval. To begin with, there is no reason to expect the limiting normal distribution to be a particularly good approximation for $n = 42$ or $T \doteq 10^{20}$. Indeed, the error terms in the normal approximation are often proportional to the standard deviations! Further, for intervals covering $\frac{1}{4}$ of the circle, the eigenvalue counts are 9, 10, 11 or 12 in most cases. Table 1 shows the eigenvalue counts for 1190 random elements of U_{42} and for the zeta data used above.

Table 1. Table of 'Eigenvalue' counts for $\frac{1}{4}$ circle based on a random sample of 1190 unitary matrices and 1190 zeta-based datasets.

Count	7	8	9	10	11	12	13	14
Unitary	0	1	79	518	496	93	3	0
Zeta function	0	2	111	485	503	87	2	0

Note that the statistics in table 1 are not just the result of density matching; both the unitary and zeta counts have some distribution on the integers and these data show that the distributions are very similar.

We carried out a chi-square test for equality of distribution between the two rows of the table. Pooling categories 8–9 and 12–13, let the table entries be $T_{i,j}$. Then $X = \sum_{j=1}^4 \frac{(T_{1,j} - T_{2,j})^2}{T_{1,j} + T_{2,j}} = 7.042$. Under the null hypothesis, X has an approximate chi-square distribution on three degrees of freedom and $P(\chi_3^2 \geq 7.042) \doteq 0.071$. This does not reject the null hypothesis 1.1.

3.5. A cautionary note

We end with a cautionary note. Recent work surveyed in [5–7] has emphasized that random matrix theory alone does not suffice to match all questions about the zeta function; some number theory must also be built in. A striking example of this is Berry's work on the variance of the number of zeros in an interval of length L , chosen at random, e.g., in $(T, 2T)$ for T large. Random matrix theory predicts that this is of order $\log L$ while Berry's formula (and data) shows it is not monotone in L . Since the variance determines the covariance by polarization, the close match in figures 8 and 9 may not hold for sufficiently large T .

4. Two further tests

To begin with, recall that according to [36], the n eigenvalues $\{e^{i\theta_1}, \dots, e^{i\theta_n}\}$ of a matrix M drawn from U_n have the following density:

$$f_2(\theta_1, \dots, \theta_n) = \frac{1}{(2\pi)^n n!} \prod_{1 \leq j < k \leq n} |e^{i\theta_j} - e^{i\theta_k}|^2. \quad (5)$$

The problem of testing the goodness of fit of the wrapped zeros to (5) with 1190 observations in 42 dimensions is akin to testing for randomness when a few balls are dropped into a huge number of boxes. Indeed, if each of the 42 coordinates was divided into two, the sample space is divided into $2^{42} \doteq 4.4 \times 10^{12}$ cells. A naive chi-square test of the hypothesis is hopeless.

It seems natural to lump the data in some cruder way. The tests in sections 2–4 accomplish this through natural statistics such as the trace and correlations.

This section constructs two further tests along classical lines. The first puts a natural one-dimensional family through the null hypothesis and tests within this family. The second is an omnibus test with power against all alternatives.

4.1. Exponential families

In the present section, the model (5) is embedded in a natural one-parameter family. Let

$$f_\beta(\theta_1, \dots, \theta_n) = \frac{\left(\frac{\beta}{2}\right)^n}{\left(\frac{n\beta}{2}\right)! (2\pi)^n} \prod_{1 \leq j < k \leq n} |e^{i\theta_j} - e^{i\theta_k}|^\beta. \quad (6)$$

This is a family of probability densities on $[0, 2\pi)^n$ for $0 \leq \beta < \infty$. When $\beta = 0$, this is the *iid* uniform measure. As β tends to infinity, it gives the picket fence model. The normalizing constant is available using Selberg's integral (Mehta [42], p 356). Of course, f_2 gives the density of unitary eigenvalues, U_n . The density f_1 arises from symmetric unitary matrices, U_n/O_n . For n even, the density f_4 arises for anti-symmetric unitary matrices, U_{2n}/SP_{2n} . Sarnak and Katz [35] have given some evidence that the zeros are related to eigenvalues of random matrices in the compact symplectic group SP_{2n} . Directly comparing along present lines is impossible since elements of SP_{2n} have eigenvalues in complex conjugate pairs. This, of course, does not occur in our data. Nevertheless, it suggests a look at $\beta = 4$. Of course, this gives the eigenvalues for the symplectic ensemble (i.e. the eigenvalues of antisymmetric unitary matrices), not the classical symplectic group.

The model (6) is a one-parameter exponential family. Lehmann [40] and Brown [9] develop the theory of exponential families, showing that optimal tests exist within this model. Accordingly, we apply the uniformly most powerful unbiased test of the hypothesis that $\beta = \beta_0 = 2$ to our data. Let $\{e^{2\pi i \theta_j^{(m)}}\}_{j=1, m=1}^{n, N}$ represent the $m = 1$ through N realizations of n 'eigenvalues' formed from the zeros data. We can write the joint density of the data under the null hypothesis as

$$\exp(\beta_0 T(\theta_j^{(m)}) - NA(\beta_0))$$

where $T = T(\theta_j^{(k)}) = \sum_{m=1}^N \sum_{1 \leq j < k \leq n} \log |e^{i\theta_j^{(m)}} - e^{i\theta_k^{(m)}}|$ and $A(\beta) = \log(\frac{n\beta!}{2}) - n \log(\frac{\beta!}{2}) + n \log(2\pi)$. By standard asymptotic theory, under f_{β_0} , T is approximately normally distributed with mean $A'(\beta_0) = 69.8616$ and variance $\frac{A''(\beta_0)}{N} = \frac{3.6042}{N} = 3.0287 \times 10^{-3}$. An approximate 1%-level test of the null hypothesis, $\beta_0 = 2$, fails to reject if and only if $T/N \in [69.72, 70.00]$. Since T/N evaluates to 69.9946 on our data, we do not reject at the 1%-level, but we do at the 5%-level; the p -value is 0.0157. The maximum likelihood value of β is 2.0375. The 99% confidence interval for β is [1.996, 2.077]. In summary, then, although we reject $\beta = 2$ at the 5%-level, we do not reject it at the 1%-level. However, we reject the alternatives $\beta = 1$ and $\beta = 4$ at all reasonable significance levels. Some further examples of this exponential family test are computed in section 6.2.

4.2. A family of consistent tests for f_2

Given $\theta^1, \theta^2, \dots, \theta^N$ in $(S^1)^n$ we construct a test $T_N(\theta^1, \dots, \theta^N)$ which is invariant under the natural symmetries of f_2 , reasonably easy to compute and consistent against all alternatives. The approximate distribution under null and alternatives is also available. The test can be represented as a sum of components which are easy to interpret. These components can also be used for adaptive versions of Neyman's smooth test, as suggested by Fan [24].

Let $\mu_N = \frac{1}{N} \sum_{j=1}^N \delta_{\theta^j}$ be the empirical measure of the data. The test statistic is

$$T_N = \int \int \prod_{j,k} (1 - z e^{i(\theta_j - \theta'_k)})^{-1} \mu_N(d\theta) \mu_N(d\theta') \quad (7)$$

with z a fixed parameter $0 < z < 1$ (e.g., $z = 0.9$).

Understanding T_N involves Schur functions $s_\lambda(x_1, \dots, x_n)$. For $\lambda = (\lambda_1, \lambda_2, \dots, \lambda_r)$ with $\lambda_1 \geq \lambda_2 \geq \dots \geq \lambda_r > 0$ a partition of $|\lambda| = \lambda_1 + \dots + \lambda_r$, s_λ is a homogeneous symmetric polynomial of degree $|\lambda|$. Here λ ranges over all partitions of all numbers with at most n parts (s_λ is zero for other partitions). For example, $s_{(0)} = 1$, $s_{(1)} = \sum x_i$, $s_{(2)} = \sum_{i \leq j} x_i x_j$, $s_{(1,1)} = \sum_{i < j} x_i x_j$. Standard references on Schur functions are MacDonalld [41] and Stanley [54].

The Schur functions are the characters of the unitary group U_n . They are orthonormal with respect to f_2 (defined in (5)):

$$\int s_\lambda(e^{i\theta_1}, \dots, e^{i\theta_n}) \overline{s_{\lambda'}(e^{i\theta_1}, \dots, e^{i\theta_n})} f_2(\theta) d\theta = \delta(\lambda, \lambda').$$

The s_λ determine weak convergence on $(S^1)^n$. That is, for a probability measure ν , we may define

$$\widehat{\nu}(\lambda) = \int s_\lambda \nu(d\theta).$$

Then, a sequence ν_k of probability measures on $(S^1)^n$ converges in the weak star topology to f_2 if and only if $\widehat{\nu}_k(\lambda) \rightarrow 0$ for each fixed $\lambda \neq (0)$. To see this, note that the set of finite linear combinations of Schur functions is a point separating algebra of continuous functions on a compact space and apply the Stone–Weierstrass theorem.

In analogy with Fourier-type tests it is natural to consider weighted combinations of $|\widehat{\mu}_N(\lambda)|^2$. The following proposition shows that an appropriate linear combinations gives T_N .

Proposition 4.1. *For any $z \in (0, 1)$, T_N defined in (7) satisfies*

$$T_N = \sum_{\lambda} z^{|\lambda|} |\widehat{\mu}_N(\lambda)|^2. \tag{8}$$

Proof. The Cauchy identity (Stanley [54], p 322) shows

$$\prod_{j,k} (1 - x_j y_k)^{-1} = \sum_{\lambda} s_{\lambda}(x) s_{\lambda}(y)$$

as formal power series. Let $x_j = z e^{i\theta_j}$, $y_k = e^{-i\theta'_k}$. Since s_{λ} is homogeneous of degree $|\lambda|$ with real coefficients, integrating the identity with respect to $\mu_N(d\theta) \times \mu_N(d\theta')$ gives

$$\int \int \prod_{j,k} (1 - z e^{i(\theta_j - \theta'_k)})^{-1} \mu_N(d\theta) \mu_N(d\theta') = \sum_{\lambda} z^{|\lambda|} |\widehat{\mu}_N(\lambda)|^2. \quad \square$$

Remark. From the equality, the infinite sum of squares converges to an almost surely finite limit.

The following proposition gives the limiting distribution of T_N under the null distribution.

Proposition 4.2. *If $\theta^1, \dots, \theta^N$ are independently drawn from f_2 .*

$$N(T_N - 1) \implies \sum_{j=1}^{\infty} z^j \text{Gamma}(p(n, j))$$

with $p(n, j)$ the number of partitions of j with at most n parts and where each $\text{Gamma}(a)$ is an independent gamma variable with density $x^{a-1} e^{-x} / \Gamma(a)$.

Proof. By the usual central limit theorem, for any fixed $\lambda \neq (0)$, $\sqrt{N} \widehat{\mu}_N(\lambda)$ converges to a mean zero standard complex normal distribution. Further, for any finite collection of λ , the limiting variates are independent. Thus, $N |\widehat{\mu}_N(\lambda)|^2$ converge to independent exponentials. The theorem follows by collecting powers of $z^{|\lambda|}$. □

We carried out the test based on $W_N = N(T_N - 1)$ with four datasets (see table 2). In each case we took $N = 1000$, $n = 42$ and $z = \frac{1}{2}$. The first dataset is a sample from Haar measure; this gives a check on our computations and on the limiting approximations. The second

Table 2. $W_N = N(T_N - 1)$ with $N = 1000, n = 42, z = \frac{1}{2}$.

Dataset	Haar on U_{42}	Zeta zeros	Picket fence	$U_{84}/2$
W_N	2.17	2.31	7.94	2.82

Table 3. $P(W_\infty \leq w_p) = p$ from proposition 4.2 with $z = \frac{1}{2}$.

p	0.05	0.10	0.25	0.50	0.75	0.90	0.95
w_p	1.58	1.72	1.99	2.35	2.82	3.35	3.75

Table 4. Expected value of $W_N = N(T_N - 1)$ under unitary, uniform and picket fence models for $n = 42, N = 1190$.

	U_n	Uniform points	Unperturbed picket fence
$z = 0.5$	2.46	4.39×10^{12}	-1189
$z = 0.9$	6.97×10^5	1.00×10^{42}	-1188
$z = 0.99$	4.8×10^{34}	1.00×10^{84}	2.80×10^{19}

dataset is the zeta data. The third dataset is the picket fence model with random perturbations, as explained at the end of section 2. The final dataset, labelled $U_{84}/2$, is explained in section 6.2.

Using proposition 4.2, we prepared table 3, which lists certain percentiles of W_∞ , the limiting approximation to W_N . This table is based on 20 000 Monte Carlo samples. More accurate approximations are available using methods described in Beran [4].

We see that the Haar dataset and the zeta dataset fall in the middle of the distribution, so this omnibus test offers no evidence for rejecting the null hypothesis. The picket fence model fails badly; recall that this model was indistinguishable from the null under the trace test. Thus the omnibus test has some discriminating power despite the high dimensions.

Remark. The numbers $p(n, j)$ are the coefficients of z^j in $\prod_{a=1}^n (1 - z^a)^{-1}$. They are thoroughly studied by Andrews [2]. From this, $\mathbf{E}W_\infty = \prod_{a=1}^n (1 - z^a)^{-1} - 1$. The expected value of W_N is not hard to compute under the uniform and picket fence models.

Under the uniform model,

$$\mathbf{E}_U(W_N) = \frac{1}{(1 - z)^n} - 1.$$

Under the picket fence model with equally spaced, *unperturbed* points,

$$\mathbf{E}_{PF}(W_N) = \frac{1}{(1 - z^n)^n} - N$$

We can see that the large N behaviour of these departures from the null hypothesis leads to very different behaviours in table 4.

The following proposition gives the asymptotic distribution of T_N under a general alternative distribution.

Proposition 4.3. *Let ν be a probability on $(S^1)^n$ which is different from f_2 . Let $\theta^1, \theta^2, \dots, \theta^N$ be independently drawn from ν . Then*

$$\sqrt{N}(T_N - \mu) \implies \text{Normal}(0, \sigma^2) \quad \text{for } N \text{ large}$$

with $\mu = \int r^2(\theta) f_2(\theta) d\theta$, $\sigma^2 = 4 \left[\int (\int r(\theta) g(\theta, \theta') f_2(\theta) d\theta)^2 \nu(d\theta') - \mu^2 \right]$ and $g(\theta, \theta') = \prod_{j,k} (1 - z^{\frac{1}{2}} e^{i(\theta_j - \theta'_k)})^{-1}$, $r(\theta) = \int g(\theta, \theta') \nu(d\theta')$.

Proof. The argument follows section 4 of Giné [26] quite closely.

From the Cauchy product,

$$g(\theta, \theta') = \sum_{\lambda} z^{\frac{|\lambda|}{2}} s_{\lambda}(\theta) \overline{s_{\lambda}(\theta')}.$$

We claim that $T_N(\theta^1, \dots, \theta^N)$ can be represented as

$$T_N = \frac{1}{N^2} \int \left| \sum_{j=1}^N g(\theta, \theta^j) \right|^2 f_2(\theta) d\theta. \tag{9}$$

For this compute

$$\left| \sum_j g(\theta, \theta^j) \right|^2 = \sum_{j,k} g(\theta, \theta^j) \overline{g(\theta, \theta^k)}.$$

Now

$$g(\theta, \theta^j) \overline{g(\theta, \theta^k)} = \sum_{\lambda, \lambda'} z^{\frac{|\lambda|+|\lambda'|}{2}} s_{\lambda}(\theta) \overline{s_{\lambda'}(\theta)} \overline{s_{\lambda}(\theta^j)} s_{\lambda'}(\theta^k).$$

Integrating with respect to $f_2(\theta)$ and using orthonormality gives

$$\int g(\theta, \theta^j) \overline{g(\theta, \theta^k)} f_2(\theta) d\theta = \sum_{\lambda} z^{|\lambda|} \overline{s_{\lambda}(\theta^j)} s_{\lambda}(\theta^k).$$

Summing over j and k gives equation (9) on the left and equation (8) on the right, proving the claim. Now, proposition (4.6) of Giné can be used to complete the result. □

To conclude this section, we mention a connection between the omnibus test based on T_N and the trace test of section 2. The normality of the trace of random unitary matrix was extended to joint normality of the trace of powers in [22] (see also Johansson [32] and Diaconis and Evans [20]). Thus, for M uniform in U_n and Borel sets $A_j \subset \mathbb{C}$. Let Φ be the standard complex normal measure (the law of $Z_1 + iZ_2$ with Z_j independent real $\text{Normal}(0, \frac{1}{2})$). The result is

$$P\{\text{tr}(M) \in A_1, \text{tr}(M^2) \in A_2, \dots, \text{tr}(M^k) \in A_k\} \rightarrow \prod_{j=1}^k \Phi(A_j / \sqrt{j}). \tag{10}$$

A variety of tests can be based on (10). As an example, consider the picket fence model introduced at the end of section 2; this has $e^{2\pi i \Theta_j}$ with $\Theta_j = \frac{i}{n} + a_n Z_j + U$, Z_j standard normal, U uniform and $a_n = \frac{1}{2\pi} \sqrt{\log \frac{n}{n-1}}$. It is easy to show that $\mathbf{E} \left| \sum_j e^{2\pi i b \Theta_j} \right|^2 = n \left(1 - \left(1 - \frac{1}{n} \right)^{b^2} \right) = b^2 \left(1 + O\left(\frac{1}{n}\right) \right)$. In contrast, the proof of (10) implies that $\mathbf{E}_{U_n} |\text{tr}(M^b)|^2 = b$. Thus, tests based on $|\text{tr}(M^b)|^2$ will reject the picket fence model for $b \geq 2$.

We now argue that tests based on equating moments of the various traces combine to give a test equivalent to the test based on T_N above. To see this, recall that the power sum symmetric

functions are defined by $P_j(x_1, \dots, x_n) = \sum_i x_i^j$ and for λ a partition $P_\lambda(x_1, \dots, x_n) = P_{\lambda_1} \cdot P_{\lambda_2} \cdots P_{\lambda_r}$. If M has eigenvalues $\{e^{i\theta_1}, \dots, e^{i\theta_n}\}$, $\text{tr}(M^j) = P_j(e^{i\theta_1}, \dots, e^{i\theta_n})$ and $\prod_{j=1}^\infty \text{tr}(M^j)^{d_j} = P_\lambda(e^{i\theta_1}, \dots, e^{i\theta_n})$, where λ has d_j parts equal to j . The Schur functions and power sum symmetric functions are linear combinations of one another. Thus, the components $\widehat{\mu}_N(\lambda)$ can be expressed as linear combinations of various moments of traces. In particular, the Cauchy product can be expanded as

$$\prod_{i,j} (1 - x_i y_j)^{-1} = \sum_\lambda \frac{1}{\xi_\lambda} P_\lambda(\mathbf{x}) P_\lambda(\mathbf{y})$$

with $\xi_\lambda = \prod_{j=1}^\infty j^{d_j} d_j!$. This gives

$$T_N = \sum_\lambda z^{|\lambda|} |\widetilde{\mu}_N(\lambda)|^2 \quad \text{where} \quad \widetilde{\mu}_N(\lambda) = \int \frac{1}{\sqrt{\xi_\lambda}} P_\lambda(\theta) \mu_N(d\theta).$$

As a further aid to understanding, we note that the components of the test statistic T_N in its two expansions can be equated in the following sense.

Proposition 4.4. *With notation as in proposition 4.3, for each $j = 0, 1, 2, \dots$*

$$\sum_{\lambda \vdash j} |\widehat{\mu}_N(\lambda)|^2 = \sum_{\lambda \vdash j} |\widetilde{\mu}_N(\lambda)|^2 \tag{11}$$

where

$$\widehat{\mu}_N(\lambda) = \frac{1}{N} \sum_{i=1}^N s_\lambda(M_i) \quad \widetilde{\mu}_N(\lambda) = \frac{1}{N} \sum_{i=1}^N \frac{P_\lambda(M_i)}{\sqrt{z_\lambda}}.$$

Proof. The argument rests on an explicit change of basis formula between the power sums and Schur functions. For λ and γ partitions of n with γ having d_i parts equal to i . Let $\chi_\lambda^{(\gamma)}$ be the character of the symmetric group S_n at the λ th irreducible and γ th conjugacy class. Let $\xi_\lambda = \prod_{j=1}^n j^{d_j} d_j!$ and $c_\lambda^\gamma = \chi_\lambda^{(\gamma)} / \xi_\gamma$. A formula of Frobenius (see chapter 1 of [41]) says that $s_\lambda = \sum_{\gamma \vdash j} c_\lambda^\gamma P_\gamma$. Then the left-hand side of (11) may be written as

$$\sum_{\lambda \vdash j} \frac{1}{N^2} \sum_{a=1}^N \sum_{b=1}^N \overline{s_{\lambda(M_a)} s_{\lambda(M_b)}} = \frac{1}{N^2} \sum_{a=1}^N \sum_{b=1}^N \sum_{\lambda \vdash j} \sum_{\gamma \vdash j} \sum_{\eta \vdash j} (\overline{c_\lambda^\gamma} c_\lambda^\eta) \overline{P_\gamma(M_a)} P_\eta(M_b).$$

After bringing the sum over λ inside, the second orthogonality relation for characters gives

$$\sum_{\lambda \vdash j} \overline{c_\lambda^\gamma} c_\lambda^\eta = \xi_\gamma^{-1} \delta_{\gamma, \eta}.$$

Thus, the left-hand side of (11) equals the right-hand side:

$$\sum_{\gamma \vdash j} \frac{1}{N^2} \sum_{a=1}^N \sum_{b=1}^N \frac{1}{\xi_\gamma} \overline{P_\gamma(M_a)} P_\gamma(M_b).$$

□

Remark. From proposition 4.3, for $j \geq 1$ and N large, the sums in proposition 4.4 have $\text{Gamma}(n, j)$ distributions under the null hypothesis.

5. Problems of dependence

Consider the tests of the trace for normality. The data of section 2 consists of W_1, \dots, W_N . Under the null hypothesis W_i has an exponential distribution. A statistic $S_N = S_N(W_1, \dots, W_N)$ was computed and S_N was calibrated under the hypothesis that W_i are exponential and *independent*. In this section we omit the hypothesis of independence and calibrate under the weaker hypothesis that W_i are exponential and stationary.

One motivation for doing this comes from computing the serial correlation:

$$\hat{\rho}_1 = \frac{\sum_{i=1}^{N-1} \left(W_i - \frac{1}{N-1} \sum_{j=1}^{N-1} W_j \right) \left(W_{i+1} - \frac{1}{N-1} \sum_{j=2}^N W_j \right)}{\sqrt{\sum_{i=1}^{N-1} \left(W_i - \frac{1}{N-1} \sum_{j=1}^{N-1} W_j \right)^2} \sqrt{\sum_{i=1}^{N-1} \left(W_{i+1} - \frac{1}{N-1} \sum_{j=2}^N W_j \right)^2}}.$$

For the data at hand, $\hat{\rho}_1 = -0.2$ indicating weak but significant negative dependence. Moore [44] and Gleser and Moore [27] give evidence that dependence can be badly confounded with goodness of fit. A second motivation comes from the wealth of experience with the Gaussian unitary ensemble (GUE) of random matrix theory. In a sequence of remarkable papers, Berry [5, 6] has argued for stationarity and a specific correlation structure. This implies that the wrapped zeros and so W_i would also be stationary. In hypothesis 5.1, we reframe the null hypothesis to allow stationarity.

The ergodic theorem implies that statistics such as A^2 will tend to zero with increasing sample size under the null hypothesis 5.1. Thus our test is asymptotically consistent, even under stationarity. Tools for calibrating the distribution of test statistics under stationarity have recently become available. We follow the development in Politis–Romano–Wolf [48]. They give extensive references to the work of Carlstein, Kunsch and many others.

Let b be a block size and let us define $S_{N,b,t}$ to be the statistic evaluated on the block $\{W_t, \dots, W_{t+b-1}\}$. The sampling distribution of S_N under the null hypothesis is approximated by

$$\hat{G}_{N,b}(x) = \frac{1}{N - b + 1} \sum_{t=1}^{N-b+1} \delta(S_{N,b,t} \leq x).$$

The critical value is then $g_{N,b}(1 - \alpha) = \inf\{x : \hat{G}_{N,b} \geq 1 - \alpha\}$ and a level- α test rejects if $S_N > g_{N,b}(1 - \alpha)$.

Politis–Romano–Wolf (theorem 3.5.1) prove that this gives an approximate level- α test under H_0 provided $N \nearrow \infty, b \nearrow \infty, b/N \rightarrow 0$. They assume the underlying stationary sequence is strongly mixing.

We carried out this test with the Anderson–Darling test statistic (2) when $N = 1190$ and $b = 35$ ($b \doteq \sqrt{N}$). The distribution of $\hat{G}_{N,b}(x)$ is shown in figure 12. For this choice of b , $g_{N,b}(0.95) = 2.2875$.

In section 9.4, Politis, Romano and Wolf suggest a data-dependent way of choosing the block size for this kind of test:

- (i) For $b = b_{\text{small}}$ to b_{big} , compute $g_{N,b}(1 - \alpha)$ as above.
- (ii) For each b compute a volatility index VI_b as the standard deviation of the values $\{g_{N,b-h}(1 - \alpha), \dots, g_{N,b+h}(1 - \alpha)\}$.
- (iii) Pick b^* corresponding to the smallest VI_b and use $g_{N,b^*}(1 - \alpha)$ as the critical value.

We choose $b_{\text{small}} = 10, b_{\text{big}} = 300$ and $h = 30$. The values $g_{N,b}(0.95)$ are shown in figure 13. The procedure gave $b^* = 106, g_{N,b^*}(0.95) = 2.28$. Finally, $S_N = 1.1050$, so we are well within the acceptance region. In contrast, the critical value of a 0.05-level test based on the Anderson–Darling statistic under independence is $g(0.95) = 2.4$.

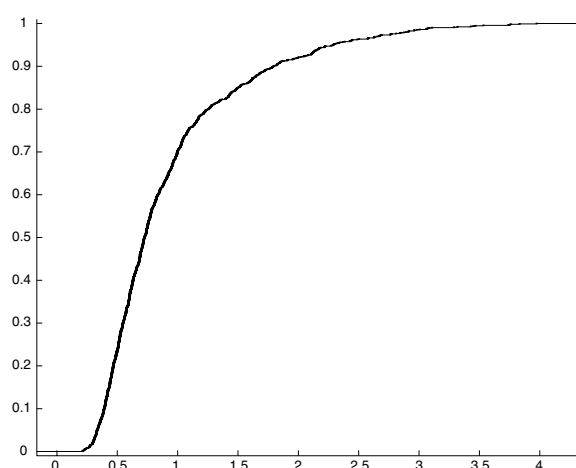


Figure 12. Approximate sampling distribution of S_N (for $b = 35$).

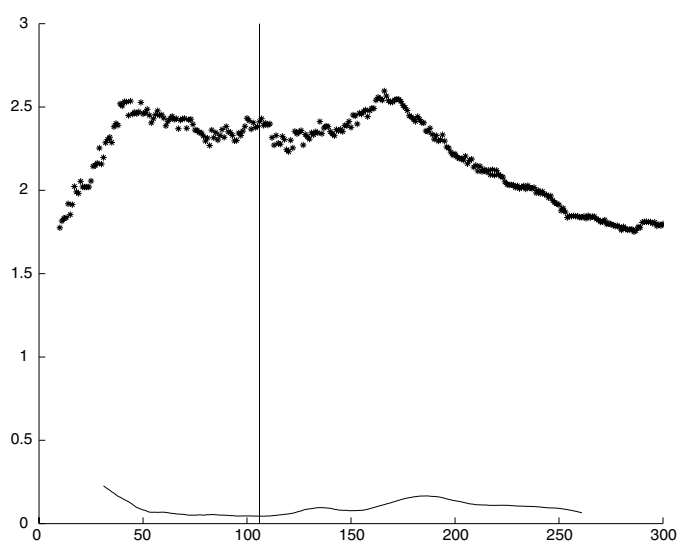


Figure 13. Graph of $g_{N,b}(0.95)$ versus b .

We conclude that, as far as traces are concerned, the zeta data fits the null hypothesis and that the stationary dependence has only a small effect on this test.

Finally, we assess the effect of dependence on the exponential family test discussed in section 4.1. Accordingly, we define

$$S_N = 2 \log \frac{\prod_{i=1}^N f_{\hat{\beta}}(\theta^i)}{\prod_{i=1}^N f_2(\theta^i)} = 2 \left[(\hat{\beta} - 2) \sum_{i=1}^N T(\theta^i) - N(A(\hat{\beta}) - A(2)) \right].$$

Here, $\hat{\beta}$ is the maximum likelihood estimate of β . On the full dataset, $\hat{\beta} = 2.0375$ and $S = 5.902$. Using the block size $b^* = 106$ as chosen above, we found

$$g_{N,b^*}(0.95) = 4.371 \quad g_{N,b^*}(0.99) = 5.7783 \quad g_{N,b^*}(0.992) = 5.9258.$$

Thus, adjusting for correlation, the null hypothesis is rejected at even the 1%-level.

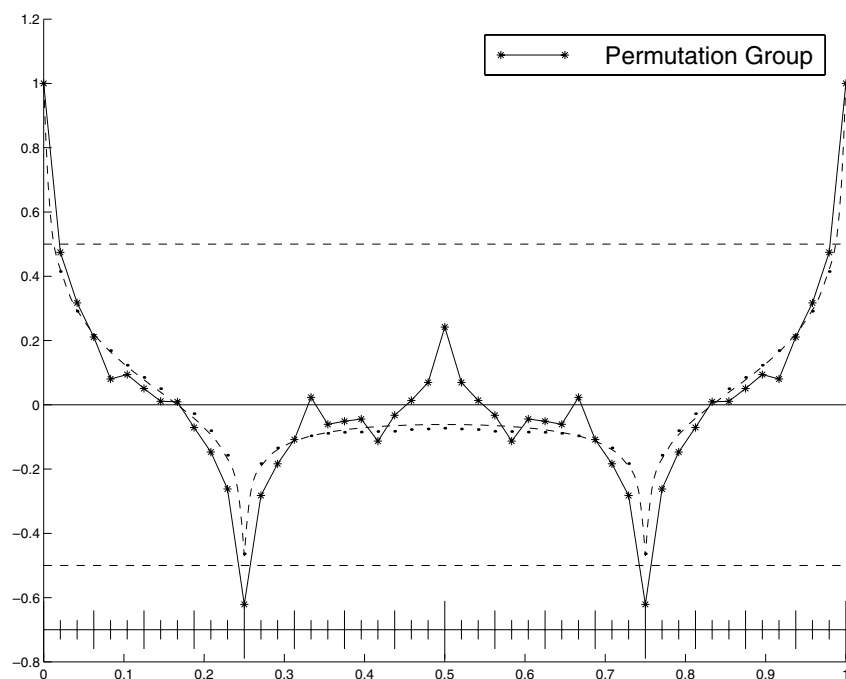


Figure 14. Permutation group, S_{42} .

The above considerations show that the lack of independence makes only a small difference. For the record, we offer a reformed hypothesis.

Hypothesis 5.1. For large T and $B = o(\sqrt{T})$, let $n = \lfloor \log \frac{T}{2\pi} \rfloor$. The $N = \lfloor (B-1)/n \rfloor$ groups of zeros, wrapped around the unit circle, form a limiting stationary process with marginal distribution equal to the eigenvalue distribution under Haar measure on U_n .

6. Remarks

6.1. Other groups

Random matrix theory is thought to apply to ‘typical’ unitary matrices in some hard to specify fairly strong sense. Mehta [42] gives further discussion.

As an example, consider the permutation group S_n in its n -dimensional representation via permutation matrices. Wieand [59] has proved that for large n , a random element of S_n has eigenvalues which obey the limiting normal distribution with correlations given by theorem 3.1. Figure 14 shows the correlations between shifted quarter circles for S_{42} . The figure has some forced extra regularities; first, the representations are orthogonal so that the eigenvalues come in complex conjugate pairs. Second, because of number theory involving cycle lengths, Wieand’s theorems only apply to intervals with irrational lengths (as opposed to quarter circles). Further developments on Wieand’s result can be found in [30].

This example shows that the correlations plots of section 3 have some discriminating ability. It reinforces our surprise at the close match shown in figures 7 and 8. We find it an

Table 5. Exponential family test results on suggestive datasets.

Dataset	$U_{84}/2$	Zeta-42	Zeta-24	Picket fence
$\hat{\beta}$	1.96	2.09	2.06	0.246
Deviance	6.44	6.71	3.27	6.4×10^4
p -value	0.011	0.0096	0.0705	≈ 0

interesting problem to prove that naturally occurring series of groups (e.g., Chevally groups) have eigenvalues close to the unitary ensemble in high-dimensional representations.

6.2. Conclusions and suggestions

This paper presents evidence of striking non-local structure in the zeros of the zeta function. Hypothesis 1.1 has been tested in two low-dimensional projections (traces and interval correlations) and in a one-parameter family. This last gives a first instance to question the validity of hypothesis 1.1.

The research reported above suggests that the unitary eigenvalues as well as the zeta data may have a self-similar structure along the following lines: consider a random matrix M in U_n with eigenvalues $\{e^{i\theta_j}\}$. Take m consecutive eigenvalues from a randomly chosen start. Wrap these eigenvalues around the circle as in section 1.1.

We hypothesize that the resulting points will be indistinguishable from Haar measure distributed points from U_m provided that both n and m are large. A test for this hypothesis using the omnibus procedure of section 4.2 with $n = 84$, $m = 42$ appears in table 2 under the name $U_{84}/2$. Using $N = 1000$ samples, the resulting omnibus test does not reject the null hypothesis.

It should be possible to prove (or disprove) this self-similarity claim, at least for the unitary group. Some related facts are now proved. Rains [49] shows that if M is chosen from Haar measure on U_{2n} , then the eigenvalues of M^2 are exactly distributed as the union of the eigenvalues of two random choices in U_n . He has similar results for higher powers and for other compact Lie groups. Forrester and Rains [25] classify matrix ensembles which have the property that if one extracts every other eigenvalue, then the result exactly follows a matrix ensemble.

We have begun to investigate the departures found with the exponential family test of section 4.1. Table 5 reports results on four fresh datasets. $U_{84}/2$ is as described above. The two zeta datasets are based on 10 000 zeros starting at about the 10^{12} th. For the first (zeta-42), the data was broken into 238 groups of size 42. For the second (zeta-24), the data was broken into 416 groups of size 24 ($T_{12} \doteq 2.67 \times 10^{11}$, so $n \doteq \log\left(\frac{T_{12}}{2\pi}\right) \doteq 24.4$). We conjecture that as T goes to ∞ , we will see β going to 2; here we have a somewhat better fit at 10^{12} but since it is based on $\frac{1}{5}$ th the data, this is not surprising. The last dataset is based on the picket fence model described at the end of section 2. The exponential family test clearly has ample power against the picket fence model. We find the results on the other datasets tantalizing, but leave their interpretation to the reader.

Acknowledgments

We thank Brad Efron for statistical suggestions; Andrew Odlyzko for the data; Dan Bump, Jon Keating and the participants of the MSRI workshop on random matrices for helpful suggestions. We also thank two referees and the editors for their careful comments.

References

- [1] Anderson T and Darling D 1952 Asymptotic theory of certain goodness-of-fit criteria based on stochastic processes *Ann. Math. Stat.* **23** 193–212
- [2] Andrews G 1976 *The Theory of Partitions* (Redding, MA: Addison-Wesley)
- [3] Bai Z 1999 Methodologies in spectral analysis of large dimensional random matrices: a review *Stat. Sinica* **9** 611–77
- [4] Beran R 1975 Tail probabilities of noncentral quadratic forms *Ann. Stat.* **3** 969–74
- [5] Berry M 1988 Semiclassical formula for the number variance of the riemann zeros *Nonlinearity* **1** 399–407
- [6] Berry M and Keating J 1999 The riemann zeros and eigenvalue asymptotics *SIAM Rev.* **41** 236–66
- [7] Bogomolny E and Keating J 1996 Random matrix theory and the riemann zeros: II. n-point correlations *Nonlinearity* **9** 911–35
- [8] Bohigas O 1991 Random matrix theories and chaotic dynamics *Chaos and Quantum Physics* ed M Giannoni, A Voros and J Zinn-Justin (Amsterdam: Elsevier)
- [9] Brown L 1986 *Fundamentals of Statistical Exponential Families* (Hayward, CA: Institute of Mathematical Statistics)
- [10] Bump D and Diaconis P 2002 Toeplitz minors *J. Comb. Theory A* **97** 252–71
- [11] Bump D, Diaconis P and Keller J 2002 Unitary correlations and the Fejér kernel *Math. Phys., Anal. and Geom.* **5** 101–23
- [12] Conrey B 2001 L-functions and random matrices *Mathematics Unlimited: 2001 and Beyond* ed B Engquist and W Schmid (Berlin: Springer)
- [13] Conrey B, Farmer D, Keating J, Rubinstein M and Snaith N 2002 Integral moments of L-functions *Preprint math.nt/0206018*
- [14] Conrey B and Gonek S 2001 High moments of the Riemann zeta function *Duke Math. J.* **107** 577–604
- [15] Costin O and Lebowitz J 1985 Gaussian fluctuations in random matrices *Phys. Rev. Lett.* **74** 69–72
- [16] D'Agostino R and Stephens M 1986 *Goodness of Fit Techniques* (New York: Dekker)
- [17] Diaconu A, Golfeld D and Hoffstein J 2001 Multiple Dirichlet series and moments of zeta and L-functions *Preprint math.nt/0110092*
- [18] Diaconis P 1988 Application of the method of moments in probability and statistics *Moments in Mathematics* ed H Landau (Providence, RI: American Mathematical Society)
- [19] Diaconis P and Efron B 1985 Testing for independence in a two-way table: new interpretations of the chi-square statistic *Ann. Stat.* **13** 845–913
- [20] Diaconis P and Evans S 2001 Linear functionals of eigenvalues of random matrices *Trans. Am. Math. Soc.* **353** 2615–33
- [21] Diaconis P and Shahshahani M 1987 The subgroup algorithm for generating uniform random variables *Probab. Eng. Info. Sci.* **1** 15–32
- [22] Diaconis P and Shahshahani M 1994 On the eigenvalues of random matrices *J. Appl. Probab.* (Special Volume) **31A** 696–730
- [23] Edwards H 1974 *Riemann's Zeta Function* (New York: Academic)
- [24] Fan J 1996 Tests of significance based on wavelet thresholding and Neyman's truncation *J. Am. Stat. Assoc.* **91** 674–88
- [25] Forrester P and Rains E 1999 Inter-relationships between orthogonal, unitary and symplectic matrix ensembles *Random Matrix Models and their Applications* ed P Bleher and A Its (Cambridge: Cambridge University Press)
- [26] Giné M E 1975 Invariant tests for uniformity on compact Riemannian manifolds based on Sobolev norms *Ann. Stat.* **3** 1243–66
- [27] Gleser L and Moore D 1983 The effect of dependence on chi-squared and empirical distribution distribution tests of fit *Ann. Stat.* **11** 1100–18
- [28] Goodman R and Wallach N 1998 *Representations and Invariants of Classical Groups* (Cambridge: Cambridge University Press)
- [29] Guhr T, Müller-Groeling A and Weidenmüller H 1998 Random matrix theories in quantum physics: common concepts *Phys. Rep.* **299** 189–425
- [30] Hambly B, Keevash P, O'Connell N and Stark D 2000 The characteristic polynomial of a random permutation matrix *Stoch. Process. Appl.* **90** 335–46
- [31] Hejhal D, Friedman J, Gutzwiller M and Odlyzko A (ed) 1999 *Emerging Applications of Number Theory* (Berlin: Springer)
- [32] Johansson K 1997 On random matrices from the compact classical groups *Ann. Math.* **145** 519–45
- [33] Johnstone I 2001 On the distribution of the largest eigenvalue in principle components analysis *Ann. Stat.* **29** 295–327

- [34] Karatsuba A and Voronin S 1991 *The Riemann Zeta Function* (Berlin: De Gruyter)
- [35] Katz N and Sarnak P 1999 *Random Matrices, Frobenius Eigenvalues and Monodromy* (Providence, RI: American Mathematical Society)
- [36] Katz N and Sarnak P 1999 Zeros of zeta functions and symmetry *Bull. Am. Math. Soc.* **36** 1–26
- [37] Keating J 1999 Random matrix theory, Lecture at *MSRI*
- [38] Keating J and Snaith N 2000 Random matrix theory and $\zeta(1/2 + it)$ *Commun. Math. Phys.* **214** 57–89
- [39] Keating J and Snaith N 2000 Random matrix theory and L-functions at $s = \frac{1}{2}$ *Commun. Math. Phys.* **214** 91–110
- [40] Lehmann E 1986 *Testing Statistical Hypotheses* 2nd edn (New York: Springer) pp 209–13
- [41] Macdonald I 1995 *Symmetric Functions and Hall Polynomials* (Oxford: Oxford University Press)
- [42] Mehta M 1991 *Random Matrices* 2nd edn (Boston, MA: Academic)
- [43] Montgomery H 1973 The pair correlation of the zeta function *Proc. Symp. Pure Math.* **24** 181–93
- [44] Moore D 1982 The effect of dependence on chi-squared tests of fit *Ann. Stat.* **10** 1163–71
- [45] Neyman J 1937 ‘Smooth’ tests for goodness-of-fit *Skand. Aktuarietidsk* **20** 149–99
- [46] Odlyzko A 1987 On the distribution of spacings between zeros of the zeta function *Math. Comp.* **48** 273–308
- [47] Odlyzko A 1999 The 10^{20} -th zero of the Riemann zeta function and 70 million of its neighbors *Technical Report* AT&T Bell Laboratories
- [48] Politis D, Romano J and Wolf M 1999 *Subsampling* (New York: Springer)
- [49] Rains E 1999 Images of eigenvalue distributions under power maps webpage <http://front.math.ucdavis.edu/math.PR/00008079>
- [50] Rudnick Z and Sarnak P 1996 Zeros of principal L-functions and random matrix theory *Duke Math. J.* **81** 269–322
- [51] Selberg A 1946 Contributions to the theory of the riemann zeta-function *Arch. Math. OG. Naturv. B* **48** 89–155 (Reprinted with commentary in the collected works)
- [52] Soshnikov A 1998 Level spacings distribution for large random matrices: Gaussian fluctuations *Ann. Math.* **148** 573–617
- [53] Soshnikov A 2000 Gaussian fluctuation for the number of particles in Airy, Bessel, sine, and other determinantal random point fields *J. Stat. Phys.* **100** 491–522
- [54] Stanley R 1999 *Enumerative Combinatorics* vol 2 (Cambridge: Cambridge University Press)
- [55] Stein C 1994 The accuracy of the normal approximation to the distribution of the traces of powers of random orthogonal matrices *Technical Report* Department of Statistics, Stanford University
- [56] Titchmarsh E 1986 *The Theory of the Riemann Zeta Function* 2nd edn (Oxford: Oxford University Press)
- [57] Verdine I and Wasserman L 1998 Bayesian goodness-of-fit testing using infinite-dimensional exponential families *Ann. Stat.* **26** 1215–41
- [58] Wieand K 1998 Eigenvalue distributions of random matrices in the permutation group and compact Lie groups *PhD Thesis* Department of Mathematics, Harvard University
- [59] Wieand K 2000 Eigenvalue distributions of random permutation matrices *Ann. Probab.* **28** 1563–87